Network Formation by Chain Polymerization of Liquid-Crystalline Monomer: A First Off-Lattice Monte Carlo Study

Devdatt L. Kurdikar,[†,‡,§] Henk M. J. Boots,[*,†] and Nikolaos A. Peppas[‡]

Philips Research Laboratories, Prof. Holstlaan 4, 5656AA Eindhoven, The Netherlands, and School of Chemical Engineering, Purdue University, West Lafayette, Indiana 47907-1283

Received December 15, 1994; Revised Manuscript Received May 10, 1995[⊗]

ABSTRACT: The first results of an off-lattice Monte Carlo simulation of network formation by chain polymerization of divinyl liquid-crystalline monomer are presented. Snapshots show the spatial inhomogeneity typical of chain reaction processes. In the present simulations the order in the nematic and smectic B phases decreases only slowly during polymerization. Due to the limited number of particles in the simulation, the radical concentation is necessarily higher than in most experiments. This expiains the small number of trapped radicals and the slow increase of the cross-link fraction as a function of conversion. The cross-link fraction is constant in the moderate-conversion region, in qualitative agreement with experiment.

Introduction

Photopolymerization of a multifunctional liquid-crystalline monomer (LCM), either in bulk or in a liquid-crystalline (LC) solvent, has been an area of both academic and industrial interest in recent years.[1,2] The (partial) fixation of the liquid-crystalline order during the polymerization leads to networks with anisotropic macroscopic properties that may be applied in a variety of optical components and LC scattering devices and in nonlinear optics.[3] Due to the ordering in the monomeric liquid, the polymerization shrinkage will be relatively low, which is favorable for applications in, *e.g.*, dentistry.[4]

Photopolymerization is used, since in that way a particular LC phase can be selected freely by the reaction temperature. In the usual way, UV radiation dissociates initiator molecules into free radicals that start a chain polymerization via the vinyl groups at both ends of the mesogenic monomer molecules.

Broer *et al.*[1] measured the birefringence of the oriented networks and demonstrated that, depending on the temperature at which the photopolymerization of such liquid-crystalline monomers is carried out, the orientational order of the molecules may either increase or decrease. Thus, at low temperatures at which the monomer is highly ordered, polymerization leads to a decrease in the ordering, probably because of increased steric hindrance effects. On the other hand, at temperatures high enough that the monomer is close to the nematic–isotropic phase transition, polymerization leads to an increased level of orientation, probably because of the increased local density in the neighborhood of particles that have reacted. The change of order during polymerization depends not only on the temperature, the density, and the LC interaction but also on the presence of lateral side groups, the length and flexibility of flexible tails on the molecules, the relative speeds of polymerization and equilibration, and the occurrence of microphase separation.

So far there have been no modeling efforts to describe such systems and to simulate the effect of temperature on the network orientation. To understand the phenomenon of ordering upon polymerization, an off-lattice model is necessary. Previous modeling efforts have been mainly lattice-based models which concentrated on describing the reaction behavior of flexible multifunctional monomers.[5–7] They are known as kinetic gelation models.[8] Lattice-based models have some inherent drawbacks. The shape and orientation of the monomer units, their mutual distances, and their dynamics can only be treated in a very restricted manner. Therefore, the development of an off-lattice model is not only important for the special case of polymerization of liquid-crystalline monomer but can also be considered as a first step toward more realism in the modeling of network formation by chain polymerization.

In this paper, we present the development and the simulation of a new three-dimensional, off-lattice, Monte Carlo technique to model the phase transition behavior of a polymerizing liquid crystal before and during polymerization.

With this model, we first prepared and studied liquid-crystalline monomer around the nematic–isotropic phase transition. Then the polymerization characteristics of rigid multifunctional monomers and the structure of the resulting networks were investigated. Preliminary results from such studies are reported. To the best of our knowledge, this is the first off-lattice model to study network formation by chain polymerization. For that reason, and because of limitations in computer time, the present model is still primitive. We feel that it will be a convenient basis for the introduction of extensions in several directions.

Simulation Technique

The simulation was constructed as a combination of two separate algorithms. The first algorithm simulated the phase transition behavior of liquid-crystalline monomer and could be used to obtain a monomer configuration at a specified temperature. The second algorithm used this configuration as an input and simulated the photopolymerization behavior.

Simulation of LCM Phase Transition Behavior. In simulating the liquid-crystalline monomer, we use the Gay–Berne[9,10] two-body interaction potential in the

[†] Philips Research Laboratories.
[‡] Purdue University.
[§] Present address: Monsanto Co., Corporate Research/Mail Zone Q3F, 800 N. Lindberg Blvd., St. Louis, MO 63167.
[⊗] Abstract published in *Advance ACS Abstracts,* July 1, 1995.

0024-9297/95/2228-5632$09.00/0

parametrization of Luckhurst *et al.*[11] (for a recent discussion on Gay–Berne parameters, see ref 12). This is an easy-to-use phenomenological potential that depends on the center positions and on the relative orientation of the interacting molecules (see Appendix A). It has a strongly repulsive core typical of ellipsoidal molecules of aspect ratio 3 and small attractive wells just outside the core. Luckhurst *et al.*[11] have shown that this phenomenological potential yields smectic, nematic, and isotropic phases.

Simulations were performed in a 3 × 1 × 1 periodic cell. A noncubic cell was chosen to reduce the effect of the finite cell size for configurations with a large director component parallel to the X direction. Such configurations are typical, even after many simulation steps, if the director in the initial configuration is chosen to be parallel to the X-axis. (This orientational preference of the director may be due to a slow disappearance of the memory of the initial orientation or to commensurability effects in the simulation.) The number of monomer units was fixed to 216, and the density was monitored by adjusting the size of the molecules. Thus, for a volume fraction of 0.5, ellipsoids with a major axis of 0.492 and a minor axis of 0.164 are used.

Though any configuration can be used at the start of the simulation, we choose for efficiency reasons an initial configuration with no overlapping repulsive cores. Each iteration step consists of the following actions.

1. A monomer molecule is selected at random.
2. With equal probability a translation or rotation move is chosen.
3. If a translation move is chosen, the center of the molecule is randomly displaced in a 0.2 × 0.2 × 0.2 cube centered at the old position of the molecule. If a rotation move is chosen, the major axis of the molecule is rotated over a random angle equally distributed in the interval [0, 10°] (the Marsaglia scheme[13,14] was adapted to apply to restricted angular intervals as described in Appendix B).
4. If the energy of the new configuration is lower, the configuration is accepted; if it is higher by an amount ΔE, it is accepted with a probability $\exp[-\Delta E/T^*]$. (Both the energy and the temperature T^* are measured in units of the Gay–Berne[9,11] energy parameter ϵ_0.) This is the well-known Metropolis criterion.[14,15]

The development of the orientational order during the simulation is followed by calculating the order parameter S, which is given by

$$S = \frac{1}{N}\sum_{i=1}^{N} P_2(\cos \beta_i) \qquad (1)$$

Here N is the number of particles, P_2 is the second Legendre polynomial, and β_i is the angle between particle i and the director. (For a thorough discussion of order parameters, see ref 16.)

Simulation of LCM Polymerization. The simulation of the polymerization process starts from a given configuration of LCM molecules. Each molecule is presumed to carry a reactive (meth)acryl group at both ends of its long axis. Initiation is simulated by converting some (in the described simulations two) reactive groups in the system to radicals. Each propagation step is followed by relaxation of the monomer unit that has been added and by relaxation of the whole system. If propagation of a radical is unsuccessful 50 times in succession, the radical is considered to be trapped. If all radicals are trapped, a new radical is created at the position of an unreacted end of a monomer unit.

A propagation step is performed as follows: An untrapped radical is selected at random and the nearest group in a box of the size of the minor ellipsoidal axis is chosen as its reaction partner. If there is no reactive group in the box, the propagation step is unsuccessful. In the reaction, the radical function is transferred to the reaction partner, and a chemical bond is formed. The Gay–Berne potential is assumed not to change during the reaction.

After a successful propagation step, the chemical bond distance will, in general, be unfavorable. If the added unit was a free monomer unit before reaction, we allow for a fast relaxation of this distance by specifically relaxing the added unit in the following way. Many (typically 10^5) times the reacted end of the unit (the pivot) is displaced by random small amounts (at most 0.01 in the $\pm X$, $\pm Y$, and $\pm Z$ directions), and the orientation of the unit is randomly changed by at most 10° according to the adapted Marsaglia scheme. Each time, if after such a move the chemical bond distance is farther away from a preset optimal value, the move is rejected; otherwise, acceptance is judged by the Metropolis criterion, using the Gay–Berne potential. In our simulations, the optimal value of the chemical bond distance was set equal to the small axis of the ellipsoidal core.

Relaxation of the system consists of a large number (10^6) of relaxation steps. In each step one chooses a monomer unit. If it is unreacted, the procedure is the same as in the simulation of pure unreacted LCM. If the unit has reacted at one side only, the procedure is similar to the case of relaxation of a unit that has just become part of the network; the only difference is that the root-mean-square chemical bond distance is used if one side of the unit is chemically attached to two units. If the unit has reacted at both sides, no moves are considered since the relaxation of cross-links is assumed to be very slow on the time scale of the simulation.

These rules are very simples ones. A wide range of variations can easily be proposed and will be tried in the future. One obvious variation would be to model the chemical bonds as Hookean springs. In that case a subtle balance between the spring energy and the repulsive interaction energy must be found: the springs must be stiff and still the units should not move into overlap to lower the spring energy.

This completes the presentation of the Monte Carlo simulation technique. This technique was designed to follow the polymerization reaction process as closely as possible. Since the orientation and the distribution of the monomer molecules were continuously followed during the reaction, we were able to study the structural evolution of the polymer network.

Preliminary Results and Discussion

Phase Transitions in LCM. In all simulations reported here, except those designed to investigate the effect of the density on the phase transition behavior, an ellipsoid volume fraction of 0.5 was used. In the starting configuration molecules with perfect X orientation were centered on the sites of a tetragonal lattice, such that the 3 × 1 × 1 periodic cell contained 6 × 6 × 6 molecules (see Figure 1).

Figure 2 shows a configuration after 10^8 iterations at a scaled temperature of $T^* = 3$. The sticks represent Gay–Berne particles, having a roughly ellipsoidal shape.

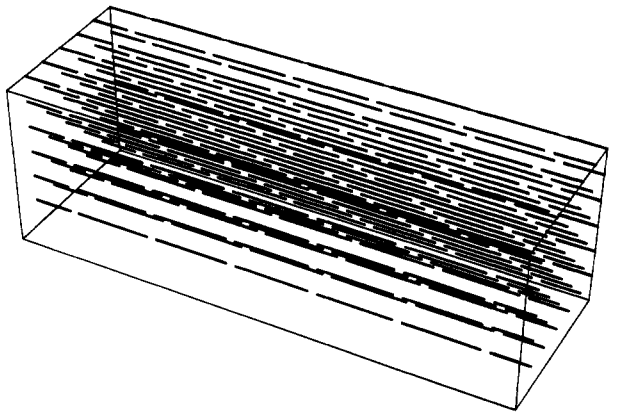

Figure 1. Fully ordered, tetragonal configuration that was used as the starting configuration to simulate the LC monomer at various temperatures. Here and below, only the major axes of the ellipsoids are drawn within the elongated cell.

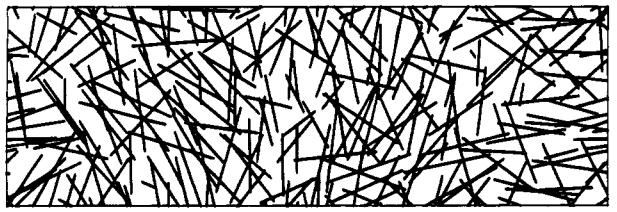

Figure 2. Configuration of LC monomer at $T^* = 3$, projected on the XY plane. The phase is isotropic.

Figure 3. Configuration of LC monomer at $T^* = 2$. The phase is nematic. The cell is viewed from a direction defined by the intersection of the XZ plane and the plane perpendicular to the director orientation.

Figure 4. Configuration $T^* = 1$, viewed from a direction perpendicular to the director orientation and parallel to a crystal direction in one of the smectic layers. The phase is smectic B.

The positional order is lost, and only some remnant nematic order may be distinguished in domains.

After 10^8 iterations at a scaled temperature of $T^* = 2$, there is no positional order and the nematic order parameter has stabilized at about 0.8. Figure 3 shows an equilibrated configuration at $T^* = 2$.

Figure 4 shows a configuration at $T^* = 1$, which was obtained after cooling from the nematic state. The configuration looks crystalline, when viewed along a crystal direction. However, the crystal direction in the middle of the simulation box is somewhat different from the crystal direction at the left and right sides of the box, as was checked from pictures at different viewing angles. Therefore, the configuration at $T^* = 1$ is smectic B, rather than crystalline. A smectic B state at low temperatures has been found before.[11]

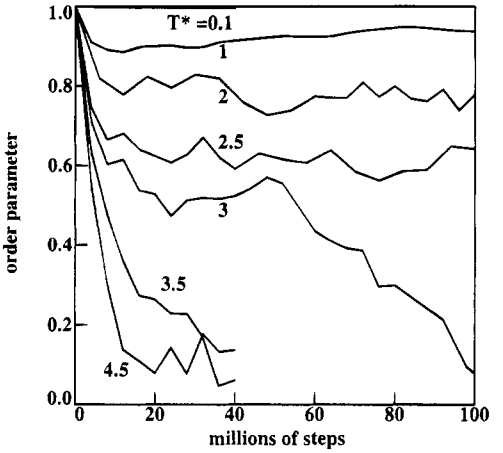

Figure 5. Order parameter as a function of the number of attempts made to move randomly chosen monomer molecules. Scaled temperatures T^* are indicated for each curve. At $T^* = 3$, the order parameter approaches zero, thus identifying the temperature of the nematic–isotropic transition.

Figure 5 shows the change in the order parameter with the number of move attempts for a range of temperatures. When simulations were carried out at T^* less than 3, the order parameters seemed to level off after 10 million move attempts and remained fairly constant over the next 90 million moves. Thus, some orientational order was retained at those temperatures and the system remained in a nematic phase. At a scaled temperature of $T^* = 3$, the order parameter approached zero after 100 million move attempts. This may be close to the temperature of the nematic–isotropic phase transition. At temperatures greater than 3, the order parameter rapidly approached zero. This figure also provides some indication that 10^8 move attempts were enough for the system to attain equilibrium as indicated by the stabilization of the order parameter.

We checked the density dependence[11,12,17] of the phases by simulations at a volume fraction of 0.28. One of the results was that at this volume fraction the system reached the isotropic phase within 10 million steps even for $T^* = 1$.

Polymerization Behavior of LCM. Using the technique outlined above, the bulk polymerization of a tetrafunctional LCM was simulated. As the initial configuration for polymerization at a certain temperature, we chose an equilibrated configuration of our Gay–Berne mesogen at that temperature. Figure 6 shows various stages of a polymerization run in the nematic state ($T^* = 2$). Note that, for clearness of presentation, the ellipsoidal particles are drawn as sticks, the unreacted molecules are left out, and the viewing direction is perpendicular to the director and parallel to the XZ plane.

At the start of the simulation, two radicals were introduced at randomly chosen ends of different monomer molecules. As the reaction proceeds, these radicals perform walks that are random but subject to restrictions: the Gay–Berne potential strongly disfavors overlap. The radical pathways, which are made up of the chemical bonds formed during the polymerization, are indicated by dashed lines. In the course of the reaction, cross-links are formed and radicals may be-

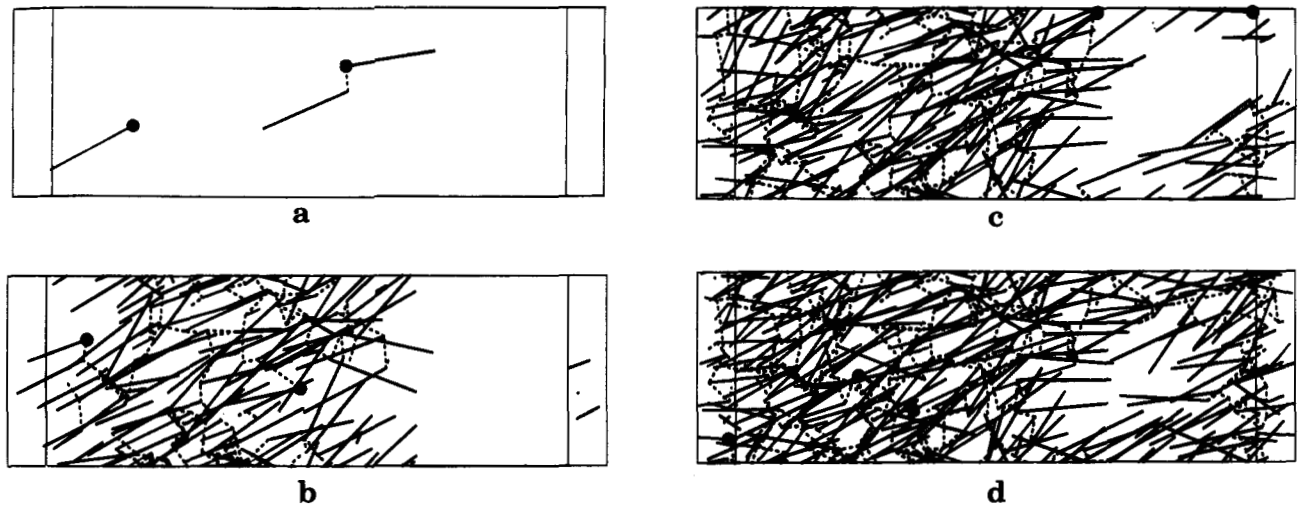

Figure 6. Configuration at $T^* = 2$ after the creation of two radicals and one reaction step of one of the radicals (a) and at conversions of 44 (b), 77 (c), and 94% (d). The viewing direction is as in Figure 3. Unreacted monomer molecules are not drawn, radical groups are indicated by filled circles, dotted lines represent the chemical bonds created during polymerization, and the ellipsoidal units are indicated by solid lines.

Figure 7. Configuration at $T^* = 3$ (projected on the XY plane) at a monomer conversion of 86%. Drawing conventions are as in Figure 2.

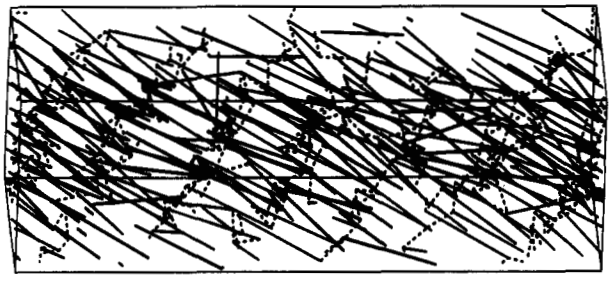

Figure 8. Configuration at $T^* = 1$ when 92% of the monomer molecules have reacted. The viewing angle is as in Figure 3; other drawing conventions are as in Figure 6.

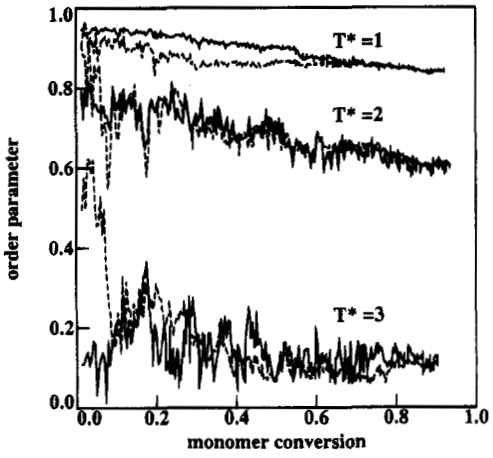

Figure 9. Order parameter of all units (drawn lines) and of polymer units (dashed lines) as a function of monomer conversion. The temperature corresponding to each pair of lines is indicated in the figure.

come trapped. If a radical gets trapped, a new one is created. In the present run, this occurred only once: at a monomer conversion of 86%. Experiments on isotropic monomer show the existence of trapped radicals at much lower conversion.[18-20] This may very well be due to the higher radical concentrations in the simulation. Like lattice model simulations, this simulation nicely illustrates the formation of temporary spatial inhomogeneity by the growing polymer chains. There is ample experimental evidence of inhomogeneity (microgel particles) during network formation by chain reactions.[21-23] If part of the monomer is replaced by unreactive molecules this inhomogeneity is still present at full conversion even without phase separation effects.

Snapshots after polymerization until a monomer conversion of about 90% are given in Figure 7 for polymerization in the isotropic state ($T^* = 3$) and in Figure 8 for polymerization in the smectic B state ($T^* = 1$). In the former case one may observe at most some local order. In the latter case both spatial and orientational order decrease somewhat during polymerization. The polymerization proceeds nicely parallel to the smectic planes. A radical may move from one plane to another at the place of a defect. In the simulation, this may also occur due to the fact that the smectic planes are not parallel to any of the cell walls: when a radical leaves the cell at one side, its periodic image will enter at the other side on a different smectic plane.

The evolution of the order parameter is depicted in Figure 9. At $T^* = 1$ and 2, the order parameter gradually decreases during the polymerization. At $T^* = 3$, the order parameter of the polymer is first higher than that of the monomer. This effect is not present in all runs. One may be tempted to explain the effect as a temporary increase in local order during polymerization. However, we feel that it is probably caused by polymerization inside an existing nematic domain. If the polymer molecule extends over many domains, the polymer order parameter averages out to the level of the order parameter before polymerization.

In simulations of chain reaction polymerization, the pendant double bond fraction, or its complement, the cross-link fraction, has obtained considerable attention. The cross-link fraction is the number of cross-link units divided by the number of all reacted units. Although

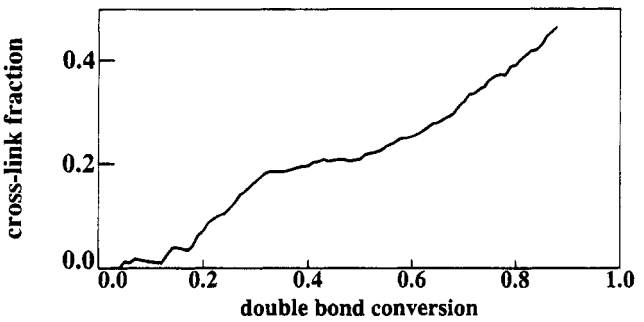

Figure 10. Cross-link fraction (the number of cross-links divided by the total number of reached units) averaged over eight polymerization runs (2 at $T^* = 1$, 3 at $T^* = 2$, and 3 at $T^* = 3$).

the experiments deal with isotropic (nonmesogenic) molecules, we feel that a qualitative comparison is still relevant. A drawback, however, is the fact that the radical concentrations in the experiments are more than an order of magnitude lower than in the present simulation. The radical concentration in the simulation can only be reduced to that level by strongly increasing the number of particles, but this would lead to unrealistic computing times. In lattice models one can handle a much larger number of particles, but in these models the nonzero volume and the dynamics of the particles can only be dealt with in a limited way.

In the experiments the cross-link fraction rises almost instantaneously to a plateau value that is maintained up to high conversions.[21,22] The high cross-link fraction early in the reaction has been ascribed to the occurrence of inhomogeneities. It is remarkable that lattice models are able to predict the steep increase of the cross-link fraction at low conversion, since this proves that the inhomogeneity that causes the effect may be explained by the chain-reaction process without invoking phase-separation phenomena. In essence, the initial increase is a one-chain phenomenon, so that it will take place in a smaller conversion range if the radical concentration is lower. Due to the high radical concentrations in the present simulation, the cross-link fraction rises only gradually to its plateau value (see Figure 10). But there is a plateau, albeit less wide than in most experiments. We interpret the plateau as a stationary situation in the growth of loosely connected microgel particles in a bath of monomer. The plateau ends when the monomer supply becomes a limiting factor. Therefore, the end point of the plateau is not expected to change if a lower initiation concentration is used.

The plateau value varies significantly between different runs. With the present statistics based on only a few runs, it is impossible to find a dependence of the plateau value on the polymerization temperature.

Conclusions

A new Monte Carlo technique to simulate network formation from liquid-crystalline monomer was presented. This off-lattice model removes the restrictions inherent to lattice models. We find smectic, nematic, and isotropic phases before polymerization. For molecules of aspect ratio 3:1, present at a volume fraction of 0.5, the nematic–isotropic phase separation was found at $T^* \approx 3$. In the present model, polymerization leads to a limited decreases of the nematic order. The inhomogeneity typical of network formation by chain polymerization is present in the snapshots. The steep increase of the cross-link fraction at low conversion is not observed due to the high radical concentration. For the same reason, radical trapping does not occur at low conversion. The preliminary results indicate the existence of a plateau in plots of the cross-link fraction as a function of conversion.

The logical next step in this work will be to scan the parameter space and to vary the prescriptions for the propagation reaction in order to understand the conditions for increase and for decrease of nematic and smectic order during the cross-linking polymerization of LC monomer. Only then will it be possible to compare the model results with the variety of experimental findings reported in the literature.

Acknowledgment. D.L.K. is grateful to Philips Research Laboratories for making the required facilities available to him during his visit. Technical discussions with Bela Mulder and Daan Frenkel (F.O.M. Institute for Atomic and Molecular Physics), with G. R. Luckhurst (University of Southampton), and with Hans Kloosterboer, Rifat Hikmet, Dick Broer, and Ingrid Heynderickx (Philips Research Labs) are gratefully acknowledged. Financial support for this work was obtained from the National Science Foundation (Grant No. CTS-93-11563) and a Global Initiative Grant from Purdue University.

Appendix A

The Gay–Berne interaction potential has been discussed in several papers[9,11] and is briefly presented here for easy reference. It has the appearance of a Lennard-Jones potential

$$U = 4\epsilon(R^{-12} - R^{-6}) \tag{2}$$

and depends on the molecular shape, the orientation $\hat{\mathbf{u}}_1$ and $\hat{\mathbf{u}}_2$, and the intermolecular vector $\mathbf{r}$ of the two interacting particles via the energy parameter ϵ and the reduced distance parameter R. The parameter R is given by

$$R = (r/\sigma_0) + 1 - \left[1 - \frac{1}{2}\chi\Phi(\hat{\mathbf{u}}_1,\hat{\mathbf{u}}_2,\hat{\mathbf{r}},\chi)\right]^{-1/2} \tag{3}$$

Here χ describes the shape anisotropy

$$\chi = [(\sigma_e/\sigma_0)^2 - 1]/[(\sigma_e/\sigma_0)^2 + 1] \tag{4}$$

and σ_e and σ_0 may be interpreted as the lengths of the long and short axes of the mesogenic molecules. The orientation dependence of R is contained in

$$\Phi(\hat{\mathbf{u}}_1,\hat{\mathbf{u}}_2,\hat{\mathbf{r}},\chi) = \frac{(\hat{\mathbf{r}}\cdot\hat{\mathbf{u}}_1 + \hat{\mathbf{r}}\cdot\hat{\mathbf{u}}_2)^2}{1 + \chi\hat{\mathbf{u}}_1\cdot\hat{\mathbf{u}}_2} + \frac{(\hat{\mathbf{r}}\cdot\hat{\mathbf{u}}_1 - \hat{\mathbf{r}}\cdot\hat{\mathbf{u}}_2)^2}{1 - \chi\hat{\mathbf{u}}_1\cdot\hat{\mathbf{u}}_2} \tag{5}$$

where $\hat{\mathbf{r}}$ is the unit vector along $\mathbf{r}$. The potential shows an unphysical attractive well within the repulsive core; in Monte Carlo simulations this feature is removed. The energy parameter is given by

$$\epsilon = \epsilon_0[1 - \chi^2(\hat{\mathbf{u}}_1\cdot\hat{\mathbf{u}}_2)^2]^{-(1/2)\nu}\left[1 - \frac{1}{2}\chi'\Phi(\hat{\mathbf{u}}_1,\hat{\mathbf{u}}_2,\hat{\mathbf{r}},\chi')\right]^{\mu} \tag{6}$$

where the parameter χ' describes the anisotropy of the well depth,

$$\chi' = [1 - \phi_\epsilon^{1/\mu}]/[1 + \phi_\epsilon^{1/\mu}] \tag{7}$$

In the present simulation we followed ref 11 in choosing

the following parameter values: $\sigma_e/\sigma_0 = 3$, $\phi_\epsilon = {}^1/_5$, $\nu = 2$, and $\mu = 1$. The parameter ϵ_0 and the temperature T only arise in the combination $T^* = \kappa_B T/\epsilon_0$, where κ_B is Boltzmann's constant.

Appendix B

By the Marsaglia scheme one can select a random orientation $\hat{\mathbf{m}}$ without using trigonometry.[13] Here we present an extension to select an orientation $\hat{\mathbf{u}}$ randomly within a cone of a given angle θ_{max} around a given orientation $\hat{\mathbf{u}}_0$. This amounts to a cos θ distribution which is a step function. A generalization to arbitrary (histogram) cos θ distributions is straightforward, but it is not of interest in the present problem.

After applying the Marsaglia scheme, we have a vector $\hat{\mathbf{m}}$ such that $\hat{\mathbf{m}}\cdot\hat{\mathbf{u}}_0$ is evenly distributed between -1 and 1 and such that the azimuthal angle of $\hat{\mathbf{m}}$ (the angle between its projection in a plane perpendicular to $\hat{\mathbf{u}}_0$ and an arbitrary vector in that plane) is evenly distributed between 0 and 2π. We want to transform it to a vector $\hat{\mathbf{u}}$ such that $\hat{\mathbf{u}}\cdot\hat{\mathbf{u}}_0$ is evenly distributed between cos θ_{max} and 1 and such that the azimuthal angle of $\hat{\mathbf{u}}$ is evenly distributed between 0 and 2π. Such a vector is found from $\hat{\mathbf{m}}$ by first determining the scalar product $(\hat{\mathbf{u}}\cdot\hat{\mathbf{u}}_0)$ from $\hat{\mathbf{m}}$, $\hat{\mathbf{u}}_0$, and the pregiven value of cos θ_{max},

$$(\hat{\mathbf{u}}\cdot\hat{\mathbf{u}}_0) = 1 - \frac{1}{2}(1 - \cos\theta_{max})(1 - \hat{\mathbf{m}}\cdot\hat{\mathbf{u}}_0) \qquad (8)$$

and by then constructing $\hat{\mathbf{u}}$ in the $\hat{\mathbf{m}}$, $\hat{\mathbf{u}}_0$ plane as

$$\hat{\mathbf{u}} = (\hat{\mathbf{u}}\cdot\hat{\mathbf{u}}_0)\hat{\mathbf{u}}_0 + [\hat{\mathbf{m}} - (\hat{\mathbf{m}}\cdot\hat{\mathbf{u}}_0)\hat{\mathbf{u}}_0][1 - (\hat{\mathbf{u}}\cdot\hat{\mathbf{u}}_0)^2]^{1/2}[1 - (\hat{\mathbf{m}}\cdot\hat{\mathbf{u}}_0)^2]^{-1/2} \qquad (9)$$

This introduces one extra calculation of a square root compared to the Marsaglia scheme. One more square-root calculation is necessary to normalize $\hat{\mathbf{u}}$. According to eq 9 $\hat{\mathbf{u}}$ remains a unit vector, but a proliferation of errors on repeated application of eq 9 may lead to deviations from unity.

If $\hat{\mathbf{m}}$ happens to be nearly (anti-) parallel to $\hat{\mathbf{u}}_0$, some special care is needed.

References and Notes

(1) Broer, D. J.; Gossink, R. G.; Hikmet, R. A. M. *Angew. Makromol. Chem.* **1990**, *183*, 45.
(2) Hikmet, R. A. M. *Adv. Mater.* **1992**, *4*, 679.
(3) Barclay, C. G.; Ober, C. K. *Prog. Polym. Sci.* **1993**, *18*, 899.
(4) Bowen, R. L. *J. Dent. Res.* **1970**, *49*, 810.
(5) Boots, H. M. J.; Pandey, R. B. *Polym. Bull.* **1984**, *11*, 415. Boots, H. M. J. *Physica* **1987**, *147A*, 90.
(6) Boots, H. M. J. In *Biological and Synthetic Polymer Networks*; Kramer, O., Ed.; Elsevier: London, 1988; p 267.
(7) Bowman, C. N.; Peppas, N. A. *Chem. Eng. Sci.* **1992**, *47*, 1411.
(8) The first papers on the kinetic gelation model focused on the critical behavior in the neighborhood of the gel point: Manneville, P.; de Sèze, L. In *Numerical Methods in the Study of Critical Phenomena*; della Dora, E., Demongeot, I., Lacolle, B., Eds.; Springer: Berlin, 1981. Hermann, H. J.; Landau, D. P.; Stauffer, D. *Phys. Rev. Lett.* **1982**, *49*, 412.
(9) Gay, J. G.; Berne, B. J. *J. Chem. Phys.* **1981**, *74*, 3316.
(10) Berne, B. J.; Pechukas, P. *J. Chem. Phys.* **1972**, *56*, 4213.
(11) Adams, D. J.; Luckhurst, G. R.; Phippen, R. W. *Mol. Phys.* **1987**, *61*, 1575. Luckhurst, G. R.; Stephens, R. A.; Phippen, R. W. *Liq. Cryst.* **1990**, *8*, 451.
(12) Luckhurst, G. R.; Simonds, P. S. J. *Mol. Phys.* **1993**, *80*, 233.
(13) Marsaglia, G. *Ann. Math. Stat.* **1972**, *43*, 645.
(14) Allen, M. P.; Tildesley, D. J. *Computer Simulation of Liquids*; Oxford University Press: Oxford, 1990.
(15) Metropolis, N.; Rosenbluth, A. W.; Rosenbluth, M. N.; Teller, A. H.; Teller, E. *J. Chem. Phys.* **1953**, *21*, 1087.
(16) Zannoni, C. In *The Molecular Physics of Liquid Crystals*; Luckhurst, G. R., Gray, G. W., Eds.; Academic Press: London, 1979. Zannoni, C. *Mol. Phys.* **1986**, *58*, 763.
(17) Frenkel, D.; Mulder, B. M. *Mol. Phys.* **1985**, *55*, 1171.
(18) Flory, P. J. *Principles of Polymer Chemistry*; Cornell University Press: Ithaca, NY, 1953; p 128.
(19) Kloosterboer, J. G.; Lijten, G. F. C. M.; Greidanus, F. J. A. M. *Polym. Commun.* **1986**, *27*, 268.
(20) Zhu, S.; Tian, Y.; Hamielec, A. E.; Eaton, D. R. *Polymer* **1990**, *31*, 154.
(21) Dušek, K.; Galina, H.; Mikeš, J. *Polym. Bull.* **1980**, *3*, 19.
(22) Kloosterboer, J. G.; van de Hei, G. M. M.; Boots, H. M. J. *Polym. Commun.* **1984**, *25*, 354.
(23) Weiss, N.; van Vliet, T.; Silberberg, A. *J. Polym. Sci., Polym. Phys. Ed.* **1979**, *17*, 2229. Kast, H.; Funke, W. *Makromol. Chem.* **1979**, *180*, 1335. Whitney, R. S.; Burchard, W. *Makromol. Chem.* **1980**, *181*, 869.

MA946334O